

Effect of carbon addition on carbide morphology of single crystal Ni-based superalloy

Zhu-huan YU¹, Lin LIU², Jun ZHANG²

1. Department of Materials Science and Engineering,
Xi'an University of Science and Technology, Xi'an 710054, China;

2. State Key Laboratory of Solidification Processing, Northwestern Polytechnical University, Xi'an 710072, China

Received 4 April 2013; accepted 10 October 2013

Abstract: Single crystal superalloys of AM3 with different carbon levels were prepared at withdraw rate of 50 $\mu\text{m/s}$. The effect of carbon addition on the carbide morphology was investigated. It was found that there were four types of MC-type carbides, acicular, nodular, blocky, and Chinese script-type in the crystals. With an increase in carbon level, the volume fraction of carbide increased significantly while the volume fraction of eutectic decreased significantly. Furthermore, the size of carbide in high level carbon alloy became much larger.

Key words: single crystal superalloy; directional solidification; carbon levels; carbide morphologies

1 Introduction

The recent re-introduction of carbon into single crystal nickel-based superalloys has been useful in reducing casting defects [1–4]. It is believed that the formation of carbides can reduce the driving force of defects [5]. Meanwhile, carbon (C) addition is also helpful in reducing oxide inclusions and surface scale [6]. Previous investigations [7] have shown that carbon additions (up to 0.125% in mass fraction) to high-refractory element content single-crystal superalloys would assist in stabilizing against the formation of thermosolutal convective instabilities during directional solidification.

The main types of carbide precipitates including MC, M_{23}C_6 and M_6C [8] have an important influence on the mechanical properties of superalloys [9]. MC carbides are usually formed during solidification process and they are major forms of carbon for the alloy [10,11]. Some recent work has reported the decomposition of primary carbides into secondary carbides such as M_{23}C_6 -type and M_6C -type due to heat treatment in similar alloy systems [12]. However, it was found that

Ta-rich MC carbides remained stable during heat treatment [13,14].

The solidification rate has great effects on carbide size and morphology with higher-rate produced finer carbides [15–17]. Also, some researches have shown the additions of elements would affect the segregation behavior of the constitutive refractory elements, and intentional carbon additions also affect the morphology of carbides [11]. Tantalum and niobium additions to superalloys alter carbide composition, but not morphology since they do not significantly affect the solidification temperature [18].

The morphology of the primary MC-type carbides would be expected to have an impact on the fluid flow and defect formation during solidification of the single crystals. However, the carbide growth rules have not been reported. Moreover, the relationship between the minor carbon addition and the carbide morphology requires further investigation, addressing relationships among carbon level, carbide growth rule and growth dynamics. Therefore, in this study, the influence of carbon on the carbide morphology of a single-crystal Ni-based superalloy and growth rule of carbides was investigated.

Foundation item: Project (51201130) supported by the National Natural Science Foundation of China; Project (2012JQ6005) supported by the Natural Science Basic Research Plan in Shaanxi Province of China; Project (SKLSP201226) supported by the Fund of the State Key Laboratory of Solidification Processing in NWPU, China; Project (11JK0805) supported by Scientific Research Program Funded by Shaanxi Provincial Education Department, China; Project (2010CV631201) supported by the National Basic Research Program of China

Corresponding author: Zhu-huan YU; Tel: +86-13891948502; E-mail: yzh0709qqy@163.com

DOI: 10.1016/S1003-6326(14)63066-1

2 Experimental

The baseline alloy used in this study was a first-generation nickel-based single-crystal superalloy AM3. Five alloys with different carbon levels were examined in this study. The chemical compositions of the experimental alloys are listed in Table 1. Single-crystal samples were prepared in a Bridgman-type directional solidification furnace by bottom seeding method. A constant withdrawal rate of 50 $\mu\text{m/s}$ was utilized. The thermal gradient was measured as 300–400 K/cm. The orientation of each single-crystal sample was determined by XRD techniques. Any sample with a misorientation of greater than 7° was considered defective and was not utilized in this study.

Table 1 Chemical compositions of experimental superalloys

No.	w(C)/ %	w(Cr)/ %	w(Co)/ %	w(Mo) /%	w(W)/ %	w(Al)/ %	w(Ti)/ %	w(Ta)/ %
1	0.001	7.87	5.50	2.31	5.10	6.06	2.12	3.55
2	0.006	7.87	5.50	2.31	5.10	6.06	2.12	3.55
3	0.045	7.87	5.50	2.31	5.10	6.06	2.12	3.55
4	0.085	7.85	5.47	2.30	5.03	6.00	2.09	3.56
5	0.150	7.85	5.47	2.30	5.03	6.00	2.09	3.56

Optical microscope (Leica DM4000M) was used to examine the microstructures and measure primary dendrite arm spacings (PDAS) and second dendrite spacings (SDAS). The as-cast samples were etched by a solution (10 mL HNO_3 + 20 mL HF + 30 mL $\text{C}_3\text{H}_8\text{O}_3$). In order to reveal the carbide morphology, a deep etching was performed using a solution containing 70% HCl and 30% H_2O_2 (volume fraction).

Scanning electron microscope (SEM) was used to examine microstructure. Secondary electron mode was used for analyzing carbide morphology. Backscattered imaging was used to quantitatively identify the composition of carbides. Carbide morphologies of the as-cast samples were examined in transverse and longitudinal planes. The carbide volume fraction and carbide size were calculated by 13×15 point grids (195 points per sample) overlaid on transverse micrographs using backscattered SEM micrographs at a magnification of 500 times. At least five fields of view were used and the average was taken.

3 Results

Similar dendrite structures were observed in all alloys with well-developed secondary arms, regardless of carbon content, as shown in Fig. 1. The increase in carbon content altered the dendrite morphology slightly, making secondary and tertiary arms more pronounced, as

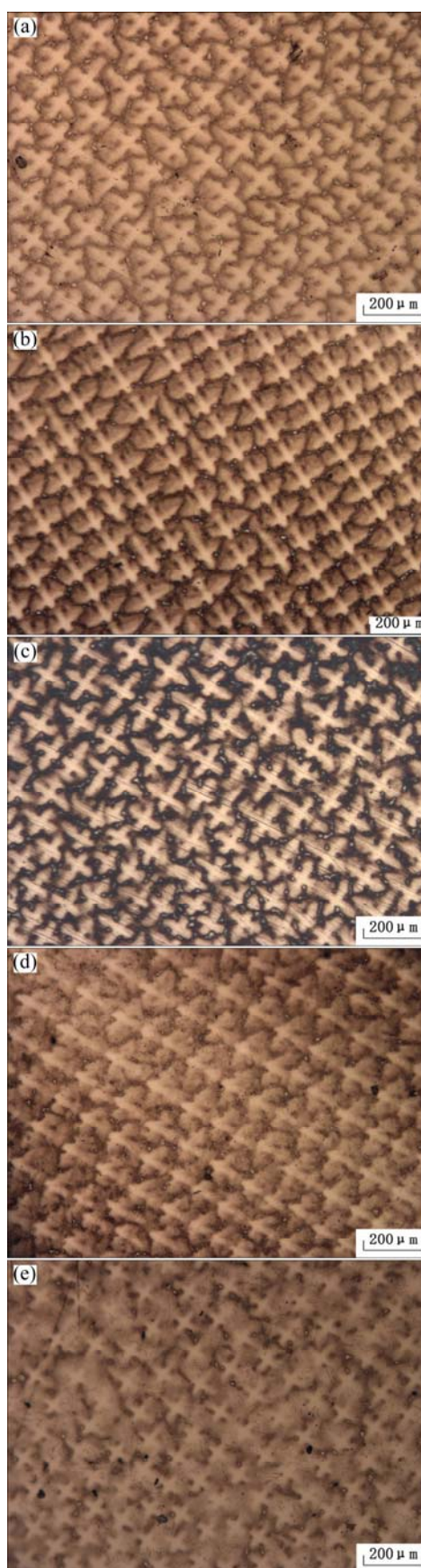


Fig. 1 Optical micrographs of as-cast dendrite microstructure for alloys with different carbon levels: (a) 0.001% C; (b) 0.006% C; (c) 0.045% C; (d) 0.085% C; (e) 0.15% C

shown in Fig. 1(e). Addition of carbon to the alloy used in this study resulted in the formation of a carbide phase in the interdendritic region of the structure, as shown in Fig. 1(d). The volume fraction of carbide phase increased with increasing the carbon content in the model alloy, as shown in Fig. 2, and carbide size also increased with increasing the carbon level (Fig. 3).

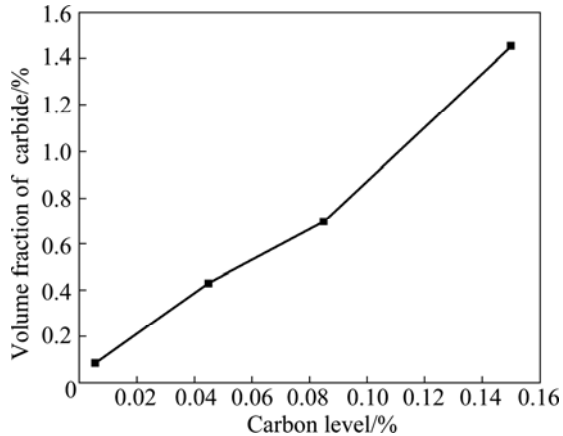


Fig. 2 Carbide volume fraction in alloys with different carbon levels (mass fraction) at withdrawal rate 50 $\mu\text{m/s}$

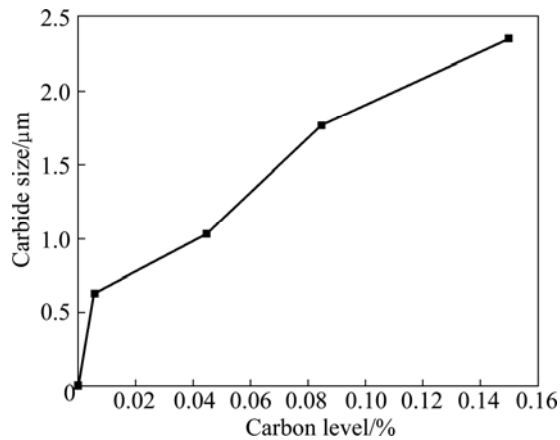


Fig. 3 Carbide size in alloys with different carbon levels (mass fraction) at withdrawal rate 50 $\mu\text{m/s}$

The micrograph of the alloy with 0.001% carbon showed large pools of eutectic, and no MC carbides were observed (Fig. 4(a)). Backscattered images showed that carbides were formed in the interdendritic regions therein other samples (Figs. 4(b), (c), (d) and (e)). MC-type carbides appeared to be bright. As the carbon content increased, an interdendritic network of carbides became more prominent. This carbide network formed alongside the dendrites during solidification. The 0.15% carbon addition showed a carbide network that grew in a “dendritic” fashion in the interdendritic region of the microstructure. Figure 4 shows that the carbide network occupied most of the interdendritic area. This result is in agreement with that in Refs. [19,20]. Some carbides also

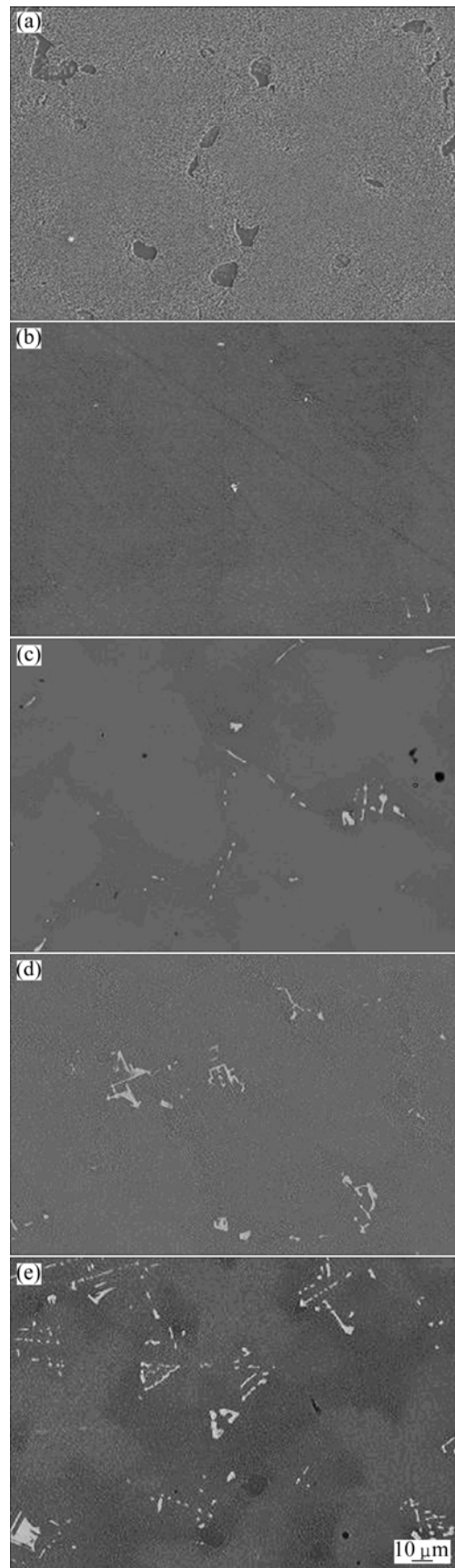


Fig. 4 Backscattered images of samples with carbides in different carbon levels: (a) 0.001% C; (b) 0.006% C; (c) 0.045% C; (d) 0.085% C; (e) 0.15% C

can be seen in the dendrite. This is because of the high carbon level, and some carbide forming elements have not enough time to form carbides in the interdendritic during the solidification process.

Figure 5 shows the carbide morphologies of deep etched sample containing 0.006% C. It can be seen that the sample contains a little carbide. The sizes of these carbides were small, and also the volume fraction of

carbides in this sample was small. This result is agreement with that of Fig. 2.

Figure 6 shows that most of the carbides in the 0.045% C alloy were blocky and sheet-like. Figure 7 reveals that the carbide morphologies were acicular in the 0.085% C alloy, sheet-like and nodular. With increasing the carbon content, the carbide morphology became Chinese-script like (Fig. 8).

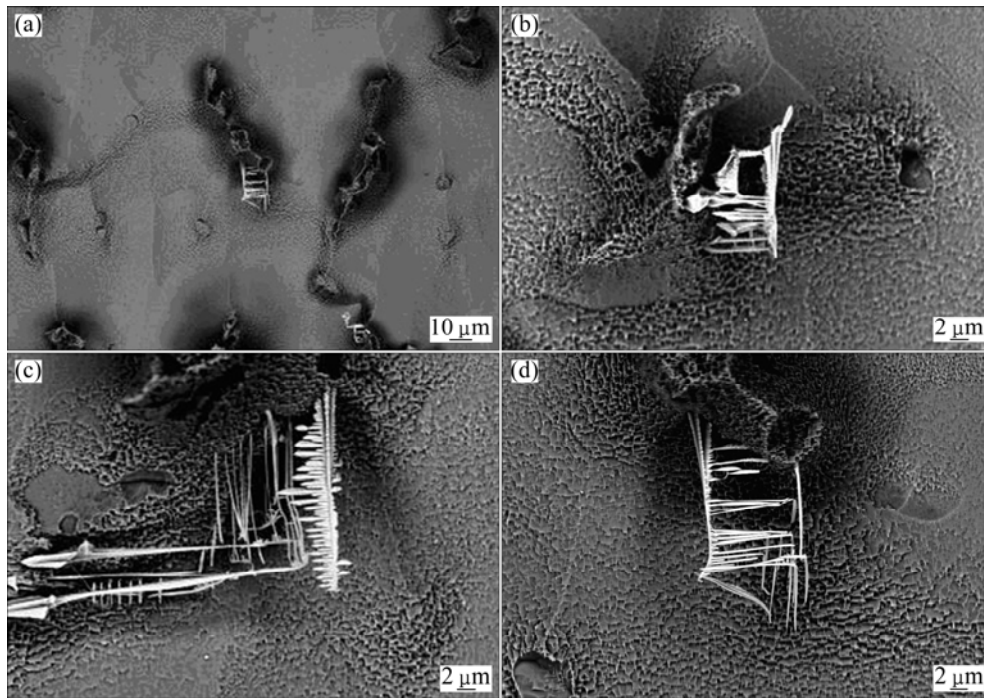


Fig. 5 SEM images showing carbide morphologies in deep etched sample containing 0.006% C: (a) Low magnification; (b) Blocky; (c, d) Acicular

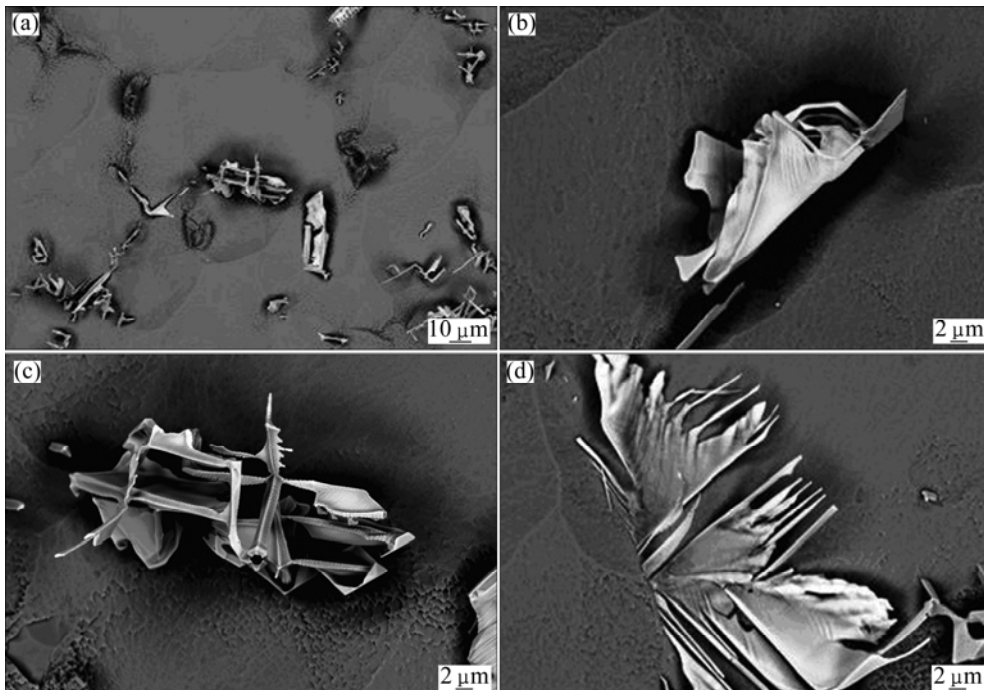


Fig. 6 SEM images showing carbide morphologies in deep etched sample containing 0.045% C: (a) Low magnification; (b, c) Blocky; (d) Sheet-like

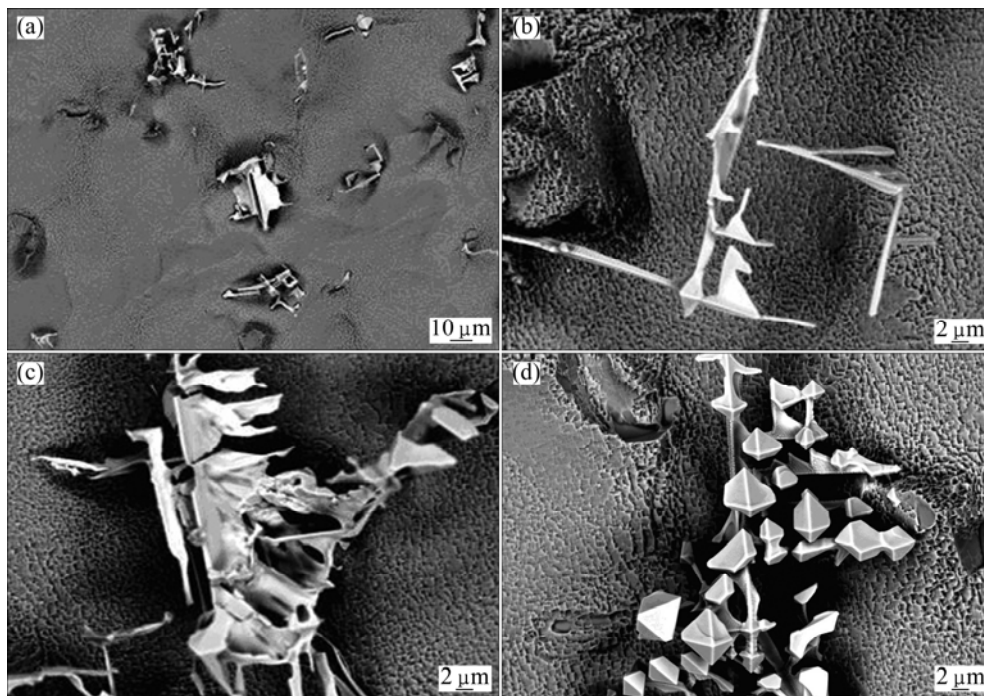


Fig. 7 SEM images showing carbide morphologies in deep etched sample containing 0.085% C: (a) Low magnification; (b) Acicular; (c) Sheet-like; (d) Nodular

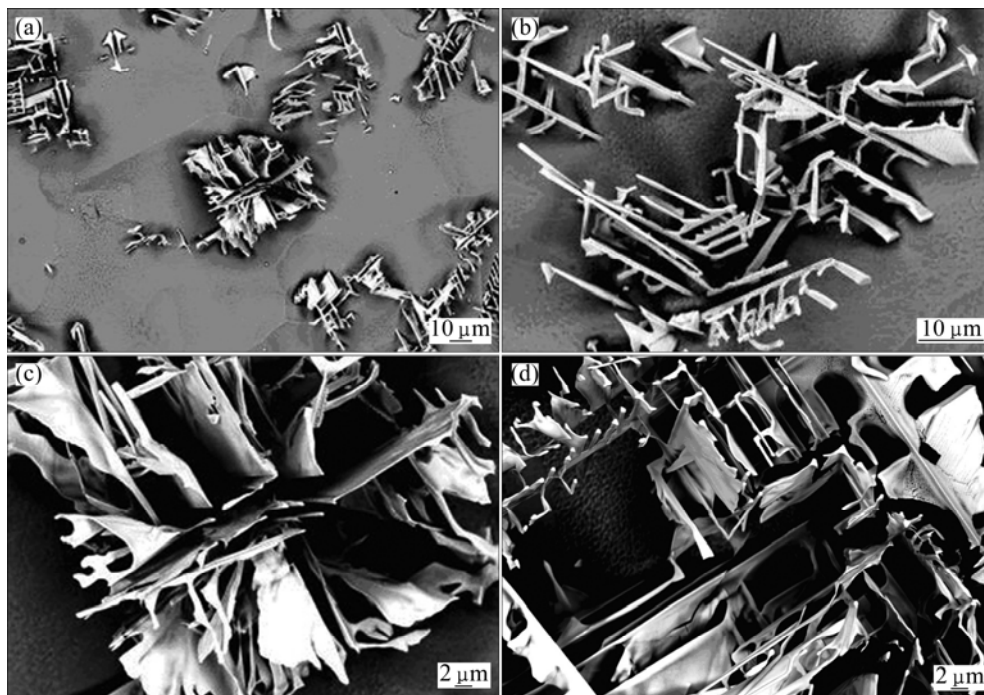


Fig. 8 SEM images showing carbide morphologies in deep etched sample containing 0.15% C: (a) Low magnification; (b,c,d) Chinese-script carbides

The carbide grown from the center was cubic dendrite shape. It can be drawn that with increasing the carbon level, the carbide size also increased. This SEM result is agreement with that in Fig. 4. Although the equilibrium morphology of carbides is octahedron based on the minimum surface energy, most of the carbides

formed in the high carbon level alloy were Chinese-script-like morphology.

Figure 8 shows that most of the carbides in the 0.15% C alloy were Chinese-script like morphology, which fully formed the carbide network in the interdendritic region. Stereo pair images of these scripts

carbide showed rods at the center of the dendritic carbides pointing out of the image. From the center, the carbides started to form in four directions starting with sheets and then splitting to form rods. These carbides grew laterally between the secondary dendrites into four directions to finally form the dendritic carbides. This observation was based on the stereo pair images in the cross sections of samples where rod-like carbides were in the center of the dendritic carbide.

A representative wavelength dispersive spectrometry spectrum is shown in Fig. 9. The result shows that all-cast carbides were Ta-rich, MC-type primary carbides. Due to the high withdraw rate of 50 $\mu\text{m/s}$ during solidification, there is not enough time for carbide forming elements to diffuse and form the equilibrium carbide morphology. As the matrix of γ and γ' forms the carbon, tantalum is rejected to the liquid and gets rich in carbide forming elements. The accumulation of carbide forming elements along with the high withdraw rate results in the formation of a complicated carbide network in the alloy. Script-like carbides of TaC were also formed in other nickel base superalloys at a withdrawal rate of 50 $\mu\text{m/s}$ [21]. In addition, as reported in literature, with the high level of carbon, volume fraction of script-like carbides is expected to be higher than that of faceted carbides at a growth rate of 18 cm/h or higher [22]. The morphologies of these carbides were also affected by the carbide precipitation temperature with respect to the liquids and solidus temperatures of the alloy.

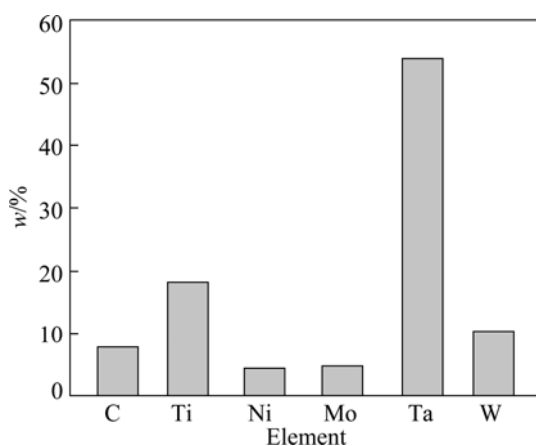


Fig. 9 Wavelength dispersive spectrometry analysis of carbide

4 Discussion

Addition of carbon to the single-crystal superalloy used in this study resulted in the formation of a carbide phase in the interdendritic region of the structure. The OM images revealed that the cast microstructures of the alloys with different carbon levels are all cruciate dendrite, which mainly contain dendrite core and

interdendritic zone. Carbides distribute mainly in interdendritic region, which indicates that the carbon-containing modifications do not significantly affect as-cast microstructure or solidification segregation, but the modifications do result in the reduction of volume fraction of eutectic and increase of carbide. The different carbon additions do result in changes in the primary dendritic carbide morphology during solidification. However, with increasing the carbon level, the volume fraction of carbide increased significantly and the volume fraction of eutectic decreased significantly. The size of carbide became large with increasing the carbon level. Meanwhile, the carbide morphology changes from acicular, nodular, and blocky to Chinese-script type with increasing the carbon addition. All as-cast carbides were Ta-rich, MC-type primary carbides.

5 Conclusions

1) The cast microstructures of the alloys with different carbon levels are all cruciate dendrite, which mainly contain dendrite core and interdendritic zone, with a great deal of irregular eutectics distributed in interdendritic zone.

2) The volume fraction of carbide in the single-crystal superalloy increases with increasing the carbon level. The average carbide size increases with increasing the carbon level. At the withdrawal rate of 50 $\mu\text{m/s}$, the carbide mainly distributes at the interdendritic zone, but also can be seen in dendrite core when the carbon level is above 2.4 μm .

3) Minor additions of carbon to single-crystal superalloy resulted in the formation of Ta-rich, MC-type interdendritic primary carbides with different morphologies. And the morphologies of carbide transform from acicular, blocky, sheet-like and nodular to Chinese-script morphology.

References

- [1] AI-JARBA K A, FUCHS G E. Effect of carbon additions on the as-cast microstructure and defect formation of a single crystal Ni-based superalloy [J]. *Materials Science and Engineering A*, 2004, 373: 255–267.
- [2] TIN S, POLLOCK T M. Carbon additions and grain defect formation in high refractory nickel-base single crystal superalloys [C]/*Proc Superalloys 2000*. Warrendale, PA: TMS, 2000: 201–210.
- [3] AI-JARBA K A. Effect of carbon additions on the microstructure and the mechanical properties of model single crystal Ni-base superalloy [D]. Florida: University of Florida, 2003: 12–14.
- [4] TIN S, LEE P D, KERMANPUR A. Integrated modeling for the manufacture of Ni-based superalloy discs from solidification to final heat treatment [J]. *Metallurgical and Materials Transactions A*, 2005, 9(36): 2493–2504.
- [5] WASSON A J, FUCHS G E. The effect of carbide morphologies on elevated tensile and fatigue behavior of a modified single crystal

- Ni-base superalloy [C]/Proc Superalloys 2008. Warrendale, PA: TMS, 2008: 489–497.
- [6] MIHALISIN J R. Some effects of carbon in the production of single crystal superalloy castings [C]/Proc Superalloys 2004. Warrendale, PA: TMS, 2004: 795–799.
- [7] TIN S. Carbon additions and grain defects formation in directionally solidified nickel-base superalloys [D]. Michigan: University of Michigan, 2001: 30–34.
- [8] WANG D, ZHANG J, LOU L H. Formation and stability of nano-scaled $M_{23}C_6$ carbide in a directionally solidified Ni-base superalloy [J]. Materials Characterization, 2009, 60: 1517–1521.
- [9] CUTLER E R. Effect of carbon additions and carbide morphology on the microstructure and mechanical properties of Ni-base superalloys [D]. Florida: University of Florida, 2006: 42–52.
- [10] YU Z H, LIU L, ZHAO X B. Effect of solidification rate on MC-type carbide morphology in single crystal Ni-base superalloy AM3 [J]. Transactions of Nonferrous Metals Society of China, 2010, 20: 1835–1840.
- [11] TIN S, POLLOCK T M. Phase instabilities and carbon additions in single-crystal nickel-base superalloys [J]. Materials Science and Engineering A, 2003, 348: 111–121.
- [12] LIU L R, JIN T, ZHAO N R. Formation of carbides and their effects on stress rupture of a Ni-base single crystal superalloy [J]. Materials Science and Engineering A, 2003, 361: 191–197.
- [13] YU J J. Effect of heat treatment on microstructure and stress rupture life of DD32 single crystal Ni-base superalloy [J]. Materials Science and Engineering A, 2007: 420–427.
- [14] CHEN Q Z, JONES N, KNOWLES D M. The microstructures of base/modified RR2072 SX superalloys and their effects on creep properties at elevated temperatures [J]. Acta Materialia, 2002, 50: 1095–1112.
- [15] WILSON B C, CUTLER E R, FUCHS G E. Effect of solidification parameters on the microstructures and properties of CMSX-10[J]. Materials Science and Engineering A, 2008, 479: 356–364.
- [16] BALDAN A. Effects of growth rate on carbides and microporosity in DS200+ Hf superalloy [J]. Journal of Materials Science, 1991, 26(14): 3879–3890.
- [17] LIU L, SOMMER F. Effect of solidification conditions on MC carbides in a nickel-base superalloy IN 738 LC [J]. Scripta Materialia, 1994, 30: 587–591.
- [18] CHEN Q Z, JONES C N, KNOWLES D M. Effect of alloying chemistry on MC carbide morphology in modified RR2072 and RR2086 SX superalloys [J]. Scripta Materialia, 2002, 47: 669–675.
- [19] LIU L R, JIN T, ZHAO N R. Effect of carbon additions on the creep properties in a Ni-based single crystal superalloy [J]. Materials Science and Engineering A, 2004, 385: 105–112.
- [20] CUTLER E R, WASSON A J, FUCHS G E. Effect of minor alloying additions on the carbide morphology in a single crystal Ni-base superalloy [J]. Scripta Materialia, 2008, 58: 146–149.
- [21] SUN W R, LEE J H, SEO A M, CHOE S J. The eutectic characteristics of MC-type carbide precipitation in DS nickel-base superalloy [J]. Materials Science and Engineering A, 1999, 271: 143–149.
- [22] BALIKCI E, MIRSHAMS R A, RAMAN A. Fracture behavior of superalloy IN738C with various precipitate microstructures [J]. Materials Science and Engineering A, 1999, 265: 50–62.

碳对镍基单晶高温合金碳化物形貌的影响

余竹焕¹, 刘林², 张军²

1. 西安科技大学 材料科学与工程学院, 西安 710054;
2. 西北工业大学 凝固技术国家重点实验室, 西安 710072

摘要: 在抽拉速率为 50 $\mu\text{m/s}$ 的条件下制备 5 种不同含碳量的单晶高温合金, 研究碳对单晶高温合金中碳化物形貌的影响。研究发现, 铸态组织中存在 4 种形貌的 MC 型碳化物, 呈针状、球状、块状以及中文汉字状。随着碳含量的增加, 碳化物的体积分数增大而共晶组织的体积显著减少。同时, 碳化物的尺寸随着碳含量的增加亦呈增大趋势。

关键词: 单晶高温合金; 定向凝固; 碳含量; 碳化物形貌

(Edited by Hua YANG)